SUPPORTING INFORMATION

Cd^{2+} as a Ca^{2+} surrogate in protein-membrane interactions: isostructural but not isofunctional

Krystal A. Morales,[†,‡] Yuan Yang,[†,‡] Zheng Long,[†] Pingwei Li,[†] Alexander B. Taylor,[§] P. John Hart,[§] and Tatyana I. Igumenova[†,*]

[†]Department of Biochemistry and Biophysics, Texas A&M University, 300 Olsen Boulevard, College Station, TX 77843, United States

[§]Department of Biochemistry and the X-ray Crystallography Core Laboratory, University of Texas Health Science Center at San Antonio, San Antonio, TX 78229, United States

Corresponding Author

*tigumenova@tamu.edu.

Author Contributions

‡These authors contributed equally.

S1. Cd^{2+} binding to the CMBL region of C2α detected by equilibrium fluorescence spectroscopy.

Cd^{2+} binding to C2α was monitored using intrinsic tryptophan fluorescence of C2α. The experiments were conducted at 25°C using an ISS Phoenix spectrofluorometer. The excitation and emission slit widths were set to 4 and 8 nm, respectively. The fluorescence emission spectra were obtained in the range from 310 to 530 nm, with the excitation wavelength of 295 nm. 10 mm quartz cuvettes were coated with Sigmacote (Sigma-Aldrich) to decrease the protein adsorption on cuvette walls.

Prior to the start of the experiments, all buffers and HPLC-grade water were treated with Chelex 100 (Sigma-Aldrich) to remove residual divalent metal ions. Concentrated stock solutions of Cd(II) nitrate were prepared in HPLC-grade water and titrated into the sample cuvette containing 0.5 μM C2α in 20 mM HEPES (pH 7.4) and 100 mM KCl. The reference cuvette contained 0.5 μM C2α in the same buffer. Instead of the metal ion solution, an equivalent volume of HPLC-grade water was added to the reference cuvette. The changes in tryptophan fluorescence emission upon Cd^{2+} binding were evident in the difference between the sample and reference spectra. Both the change in the emission intensity and the shift of the emission maximum were observed over the course of the titration experiment. To quantify the Cd^{2+} binding process, we calculated the spectral center of mass (CM)[1] of the emission spectra at each metal ion concentration. The change in CM divided by the maximum observed change upon Cd^{2+} saturation of CMBL sites is proportional to the fraction of the Cd^{2+}-complexed C2α, F_{Cd}. The data were fitted with the Hill equation:

$$F_{Cd}=\frac{[M^{2+}]^{H}}{[M^{2+}]_{1/2}{}^{H}+[M^{2+}]^{H}}$$

where H is the Hill coefficient, and $[M^{2+}]_{1/2}$ is the Cd^{2+} concentration required to yield the half-maximal CM change. The fit produced the following parameters: H=2.9 ± 0.3 and $[M^{2+}]_{1/2}$ =1.1 ± 0.1 μM. The low-affinity Cd^{2+} site (*vide infra*) is not appreciably populated at the 0.5 μM C2α concentration used in the fluorescence experiments.

S2. Cd^{2+} binding to C2α detected by NMR spectroscopy.

A. Sample preparation and NMR experiments.

Uniformly ^{15}N-enriched C2 domain (residues 155-293 of Protein Kinase Cα from *R. norvegicus*) was over-expressed and purified to homogeneity as previously described.[2] The protein solution was prepared at the concentration of 110 μM in NMR buffer containing 10 mM 2-(N-morpholino) ethanesulfonic acid (MES) at pH = 6.0, 8% D_2O, and 0.02% NaN_3. The stock solutions of Cd(II) nitrate were prepared in the same buffer. Aliquots of Cd(II) nitrate stock solution were added stepwise to the uniformly ^{15}N-enriched C2α. The Cd^{2+}-binding and assignment experiments were conducted on a Varian Inova spectrometer operating at the Larmor ^1H frequencies of 500 and 600 MHz, respectively. The temperature in the NMR experiments was maintained at 25 °C. The resonances of Cd^{2+}-complexed C2α were assigned using: (i) 3D HNCACB experiment with ^2H decoupling[3] that was carried out on fractionally deuterated, [U-^{13}C,^{15}N] enriched C2α in the presence of 15-fold molar excess of Cd^{2+}, (ii) the titration behavior of the individual cross-peaks, and (iii) the previously obtained assignments of apo and Ca^{2+}-bound C2α.[2]

For the chemical shift perturbation (CSP) analysis, the overall change in chemical shift Δ was calculated between a pair of protein states as:[4]

$$\Delta=[(\Delta\delta_H)^2+(0.152\Delta\delta_N)^2]^{1/2}$$

where $\Delta\delta_H$ and $\Delta\delta_N$ are the differences between the ^1H_N and ^{15}N chemical shifts of the two states being compared.

B. Binding of Cd3 to C2α.

The affinity of Cd^{2+} ions to the CMBL region of C2α could not be estimated based on the NMR data, because the binding kinetics fall into the intermediate-to-slow exchange regime. As an alternative, we used fluorescence spectroscopy (*vide supra*). However, the fast exchange behavior of the N-terminal/Helix3 region enabled us to estimate the dissociation constant of the third Cd^{2+} ion, Cd3, using NMR. The binding curves were constructed by plotting a combined change in ^1H_N and ^{15}N chemical shifts Δ against total Cd^{2+} concentration. All curves have a slight lag period because the higher-affinity CMBL sites get populated first. This and the changes in the millisecond-timescale dynamics of the protein upon binding metal ions (K. A.

Morales and T.I. Igumenova, unpublished data) make it difficult to construct an analytical function that accurately describes the binding process. To estimate the binding affinity, we simply fit the residue-specific curves individually with the Hill equation, corrected for the free ligand concentration, as described for the C2 domain of rabphilin-3A.[5] The range of apparent K_d values is 270-1100 μM, with the mean of 540 μM. The binding curves are given in **Figure S1**.

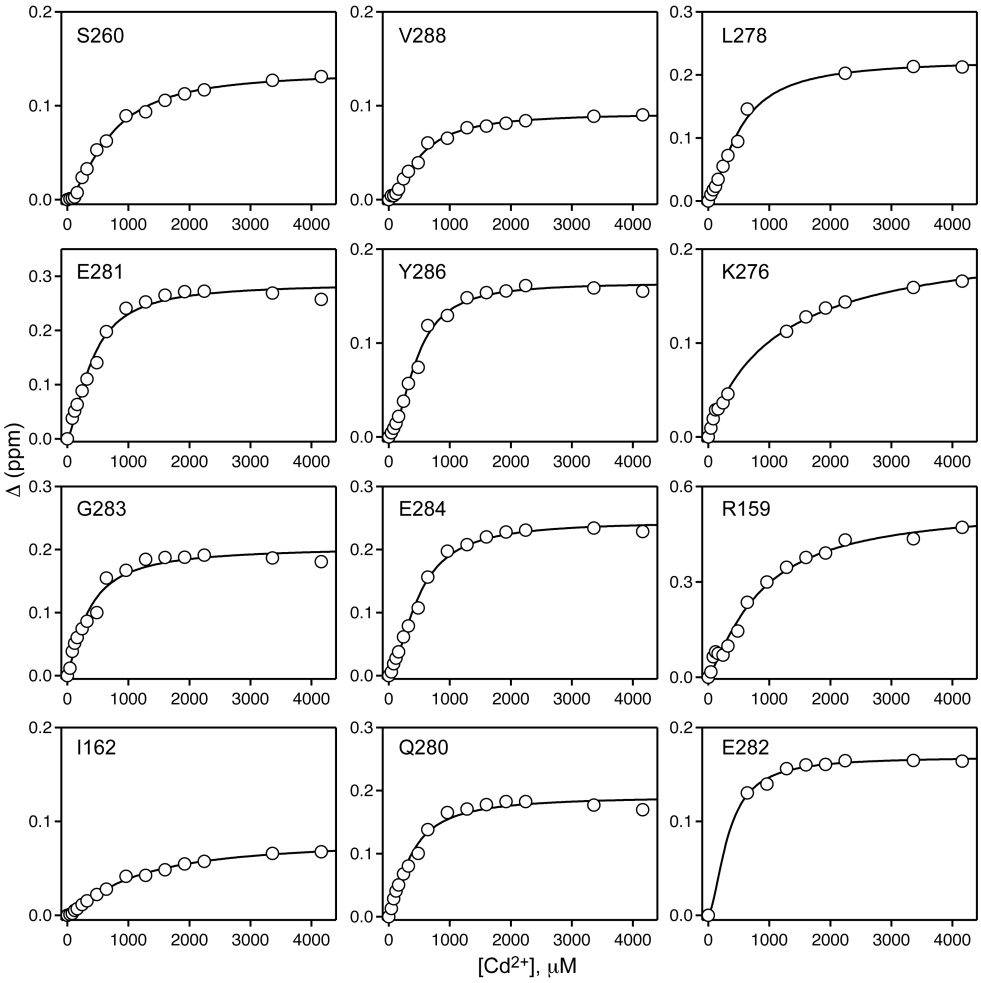

Figure S1. NMR-detected Cd^{2+}-binding curves of C2α. The solid lines represent the fits to Eq. (3) of Montaville et al.[5] Missing data points at certain Cd^{2+} concentrations indicate that the corresponding cross peak is not resolved in the HSQC spectrum.

S3. Crystallization, structure determination, and refinement of Cd^{2+}-complexed C2α.

A. Crystallization and structure determination of Cd^{2+}-complexed C2α.

The Cd^{2+}·C2α complex was crystallized using the hanging drop vapor diffusion method. C2α at 24 mg/mL was pre-incubated with a 9-fold molar excess of Cd(II) nitrate at 16 °C and mixed with the precipitant solution in a 1:1 ratio. The precipitant was 0.25 M lithium sulfate monohydrate and 20% PEG 3350, in 50 mM Bis-Tris buffer at pH 5.25. Hexagonal-shaped crystals appeared within one week and were allowed to grow for two more weeks at 16 °C.

X-ray diffraction data were collected using a Rigaku RAXIS IV++ image plate detector mounted on a Rigaku Micromax-007HF generator. The data were processed with XDS.[6] The Cd^{2+}·C2α complex crystallized in space group $P3_221$ with cell parameters $a=b=58.2$ Å and $c=88.5$ Å, and one C2α molecule in the asymmetric unit (AU). Experimental phases were obtained using the single-wavelength anomalous diffraction (SAD) method, with Cd as the anomalous scatterer. The initial model was adjusted with O[7] and Coot[8], and refined with the PHENIX program suite.[9] The coordinates were deposited into the Protein Data Bank (http://www.pdb.org/) with ID code of 4L1L.

Table S1. Data collection and refinement statistics.

Data collection	
Space group	$P3_231$
a, *b* (Å)	58.2
c (Å)	88.5
Resolution range (Å)[a]	44.3-1.60 (1.69-1.60)
Wavelength (Å)	1.54178
Redundancy	20.0 (17.8)
Completeness (%)	98.7 (94.3)
$I/\sigma I$	22.4 (7.2)
R_{sym} (%)[b]	9.8 (37.6)
Wilson value	20.0
Refinement	
R_{cryst} (%)[c]	15.7
R_{free} (%)[d]	19.5
Rmsd bonds (Å)	0.010
Rmsd angles (°)	1.225
Ramachandran outliers (%)[e]	0.0
No. protein atoms	1,172
No. solvent atoms	141
No. ligand atoms (6 Cd, 5 SO_4)	31
Avg. protein B-factors (Å^2)	25.7
Avg. solvent B-factors (Å^2)	36.4
Avg. ligand B-factors (Å^2)	35.7

[a]The number in parentheses is for the highest resolution bin. [b]$R_{sym} = \sum_{hkl}|I - \langle I\rangle|/\sum_{hkl}\langle I\rangle$ where I is the observed intensity and $\langle I\rangle$ is the average intensity of multiple symmetry-related observations of that reflection. [c]$R_{cryst} = \sum_{hkl}\big||F_{obs}| - |F_{calc}|\big|/\sum_{hkl}|F_{obs}|$. [d]$R_{free} = \sum_{hkl}\big||F_{obs,t}| - |F_{calc}|\big|/\sum_{hkl}|F_{obs,t}|$ where $|F_{obs,t}|$ is from a test set not used in the structural refinement. [e]Ramachandran plots were calculated using Coot.

B. Analysis of the Cd^{2+}-complexed C2α structure.

Table S2. Cd-O distances in Cd^{2+}-complexed C2α structure.

Cd1 CN[a]=7	Bond length (Å)	Cd2 CN=7	Bond length (Å)	Cd3 CN=6	Bond length (Å)
D187 (Oδ1)	2.57	D187 (Oδ1)	2.45	E157 (Oδ2)	2.62
D187 (Oδ2)	2.52	D248 (Oδ2)	2.67	E282 (Oδ2)	2.67
D193 (Oδ2)	2.35	D248 (Oδ1)	2.55	E282 (Oδ1)	2.59
D248 (Oδ1)	2.40	D254 (Oδ2)	2.45	N279 (Oδ1)	3.04
D246 (Oδ1)	2.35	D246 (Oδ2)	2.34	H_2O (141)	2.84
W247 (O)	2.36	M186 (O)	2.53	H_2O (142)	2.20
H_2O (10)	2.46	H_2O (43)	2.54		
Average	2.43±0.09		2.50±0.10		2.66±0.28

[a]CN stands for coordination number

Table S3. The coordination geometry of Cd^{2+} complexed to the CMBL region of C2α is pentagonal bipyramidal.

Cd1	Angle (°)	Cd2	Angle (°)
H_2O (10)-**Cd1**-W247 (O)	93.8	H_2O (43)-**Cd2**-D248 (Oδ1)	96.6
H_2O (10)-**Cd1**-D193 (Oδ2)	**80.6**	H_2O (43)-**Cd2**-D248 (Oδ2)	**80.5**
H_2O (10)-**Cd1**-D187 (Oδ2)	94.4	H_2O (43)-**Cd2**-M186 (O)	79.7
H_2O (10)-**Cd1**-D187 (Oδ1)	80.9	H_2O (43)-**Cd2**-D254 (Oδ2)	98.3
H_2O (10)-**Cd1**-D248 (Oδ1)	81.0	H_2O (43)-**Cd2**-D187 (Oδ1)	81.3
D246 (Oδ1)-**Cd1**-W247 (O)	83.8	D246 (Oδ2)-**Cd2**-D248 (Oδ1)	84.3
D246 (Oδ1)-**Cd1**-D193 (Oδ2)	**106.2**	D246 (Oδ2)-**Cd2**-D248 (Oδ2)	**110.5**
D246 (Oδ1)-**Cd1**-D187 (Oδ2)	90.9	D246 (Oδ2)-**Cd2**-M186 (O)	94.0
D246 (Oδ1)-**Cd1**-D187 (Oδ1)	98.2	D246 (Oδ2)-**Cd2**-D254 (Oδ2)	93.6
D246 (Oδ1)-**Cd1**-D248 (Oδ1)	91.3	D246 (Oδ2)-**Cd2**-D187 (Oδ1)	84.7
Average	90.1±8.5	Average	90.3±10.0

The angles were measured from the four axial ligands (2 per Cd site) to the equatorial ligands (**Figure S2A**). The average angle is 90 degrees. Four equatorial ligands belong to the same plane, while the fifth equatorial ligand is slightly out-of-plane (**Figure S2B**).

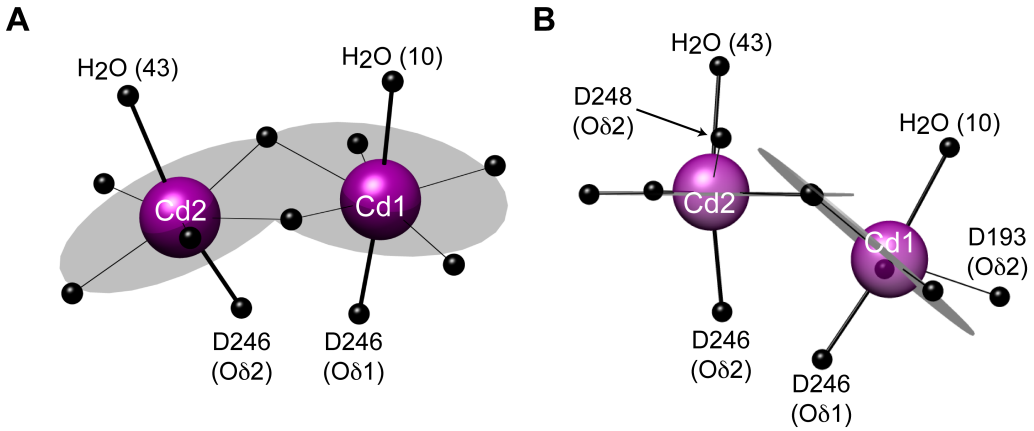

Figure S2. The geometry of Cd^{2+} coordination in the Cd^{2+}-complexed C2α structure. (A) Axial ligands used for the angle measurements. (B) The relative orientation of the planes formed by the equatorial ligands. Axial and out-of-plane equatorial ligands are labeled.

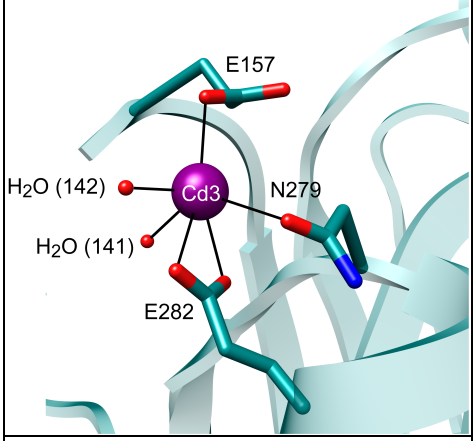

Figure S3. Coordination geometry of the Cd3 site in the Cd^{2+}-complexed C2α.

C. Two out of three low-affinity Cd^{2+} sites are in the CMBL region.

In addition to Cd1, Cd2, and Cd3, the crystal structure of the Cd^{2+}-complexed C2α has three more Cd^{2+} ions. These sites are not appreciably populated in the NMR-detected binding experiments (Section S2) and are low-affinity. Each of them has < 4 protein ligands. One Cd^{2+} ion is coordinated by the two side-chain oxygen atoms of the Glu265 sidechain and 3 water molecules. The other two Cd^{2+} ions are located in the CMBL region; their coordination geometry is shown in **Figure S4**.

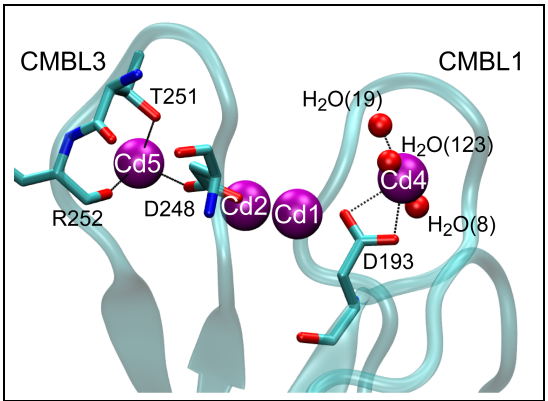

Figure S4. Coordination geometry of Cd4 and Cd5 complexed to the CMBL region.

D. Cd^{2+} binding to C2α does not alter the backbone conformation.

Table S4. Backbone root-mean-square deviation (RMSD) of the available C2α structures from the Cd^{2+}-complexed C2α structure.

PDB ID	C2α state	Resolution (Å)	RMSD (bb atoms, Å)	Ref.
4L1L	Cd^{2+}-complexed	1.6	0	This work
3RDJ	apo	1.9	0.310	[2]
1DSY	Ca^{2+}- & PSF[a]-complexed	2.6	0.325	[10]
3TWY	Pb^{2+}-complexed	1.5	0.220	[2]

[a]PSF stands for 1, 2-dicaproyl-sn-phosphatidyl-L-serine

S4. Comparison of chemicals shifts for the Ca^{2+}- and Cd^{2+}-bound states of C2α.

A comparison of the CSP values for the (Cd^{2+}-apo) and (Ca^{2+}-apo) pairs shows that the regions that differ most are the C- and N-termini, and the CMBL3 (**Figure S5**). The former is due to the binding of the Cd3 ion. The latter is likely due to the unequal Ca^{2+} and Cd^{2+} occupancies of the low-affinity CMBL3 metal binding site (see Cd5 in **Figure S4**) that is weakly populated at high concentrations of metal ions. Differences in the μs-to-ms dynamics of the CMBL3 region in Ca^{2+} and Cd^{2+}-bound C2α may also contribute to the differences in CSP values.

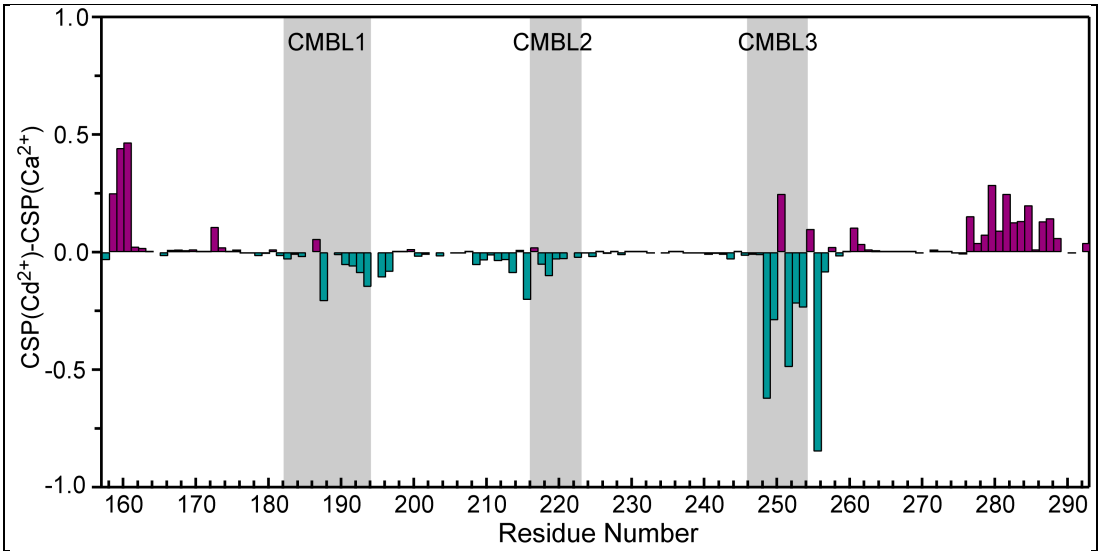

Figure S5. The difference of the CSP values for the (Cd^{2+}-apo) and (Ca^{2+}-apo) pairs. The concentration of metal ions is 4.16 mM (Cd^{2+}) and 2.78 mM (Ca^{2+}); the concentration of C2α is 100 μM. The CMBL regions are defined as: CMBL1 (182-193), CMBL2 (216-222), and CMBL3 (246-253).

S5. Metal-ion-dependent membrane association of C2α monitored using Förster Resonance Energy Transfer (FRET).

Metal ion-dependent membrane association of C2α was monitored by FRET between the tryptophan residues of C2α and the fluorescent lipid, dansyl-PE, as described previously.[2,11] The composition of large unilamellar vesicles (LUVs) was POPC/POPS/dansyl-PE (73:20:7). POPC (1-palmitoyl-2-oleoyl-sn-glycero-3-phosphocholine), POPS (1-palmitoyl-2-oleoyl-sn-glycero-3-phospho-L-serine); and dansyl-PE (1,2-dioleoyl-sn-glycero-3-phosphoethanolamine-N-(5-dimethylamino-1-naphthalenesulfonyl) were purchased from Avanti Polar Lipids (Alabaster, AL). The total concentration of lipids was 150 μM.

Aliquots of stock solutions of metal ion salts, Ca(II) chloride or Cd(II) nitrate, were added in parallel to the sample and reference cuvettes. The sample cuvette contained a mixture of 0.5 μM C2α and 150 μM LUVs in 20 mM HEPES buffer (pH 7.5) and 100 mM KCl. The reference cuvette contained all the same component but the protein. Protein-to-membrane FRET was monitored as the change in the intensity of the dansyl emission band in the difference spectra.

To determine if Cd^{2+} can directly quench the fluorescence of the dansyl group, we monitored the dansyl fluorescence emission band of the LUVs at increasing concentration of Cd^{2+} ions. **Figure S7** shows that at Cd^{2+} concentrations used in our FRET experiments no appreciable quenching of dansyl fluorescence is observed.

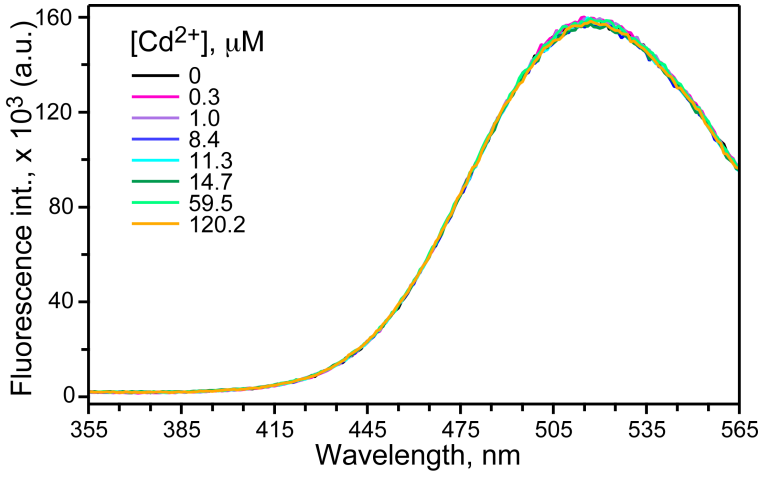

Figure S6. Cd^{2+} does not quench the fluorescence of membrane-embedded dansyl group. The spectra were obtained using the excitation wavelength of 295 nm.

S6. Cd^{2+} does not interact with PtdSer-containing LUVs under conditions of our experiments.

The interaction of Cd^{2+} with the PtdSer-containing LUVs was characterized using ultracentrifugation lipid-binding assays. The assays were carried out as previously described,[2] at a total lipid concentration of 1.5 mM but without C2α. The sucrose-loaded LUVs comprising POPC/POPS (80:20) were incubated with Cd^{2+} at different concentrations and then subjected to ultracentrifugation. The concentration of Cd^{2+} in the supernatant fraction was determined using the fluorescence-based Leadmium™ kit (Invitrogen). A plot of [Cd^{2+}] concentration in the supernatant versus total [Cd^{2+}] shows that virtually no interaction occurs between Cd^{2+} and LUVs up to 500 μM total Cd^{2+} (**Figure S7**).

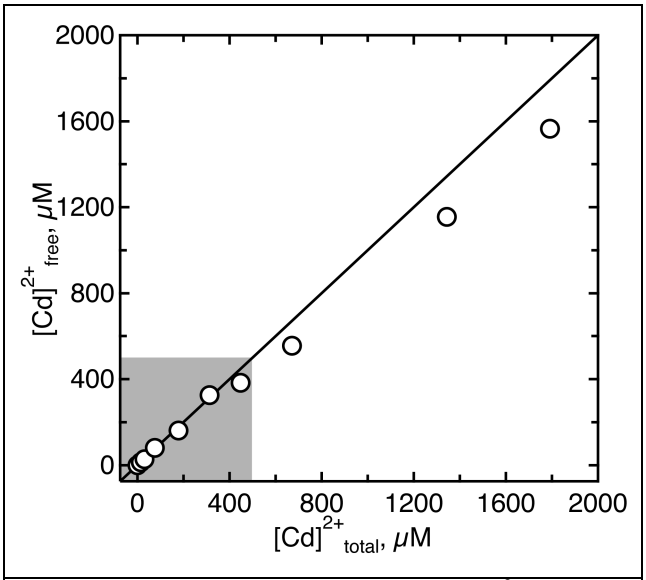

Figure S7. A plot of free versus total Cd^{2+} concentration showing negligible interactions between Cd^{2+} and PtdSer-containing LUVs up to 500 μM of Cd^{2+}.

S7. NMR-detected Cu^{2+}-binding studies of C2α.

The NMR-detected Cu^{2+}-binding experiments were carried out as described for Cd^{2+}. The paramagnetic relaxation enhancement (PRE) was calculated as the ratio of cross-peak intensities of the apo and Cu^{2+}-complexed [U-^{15}N] enriched C2α. The results are summarized in **Figures S8** and **S9**.

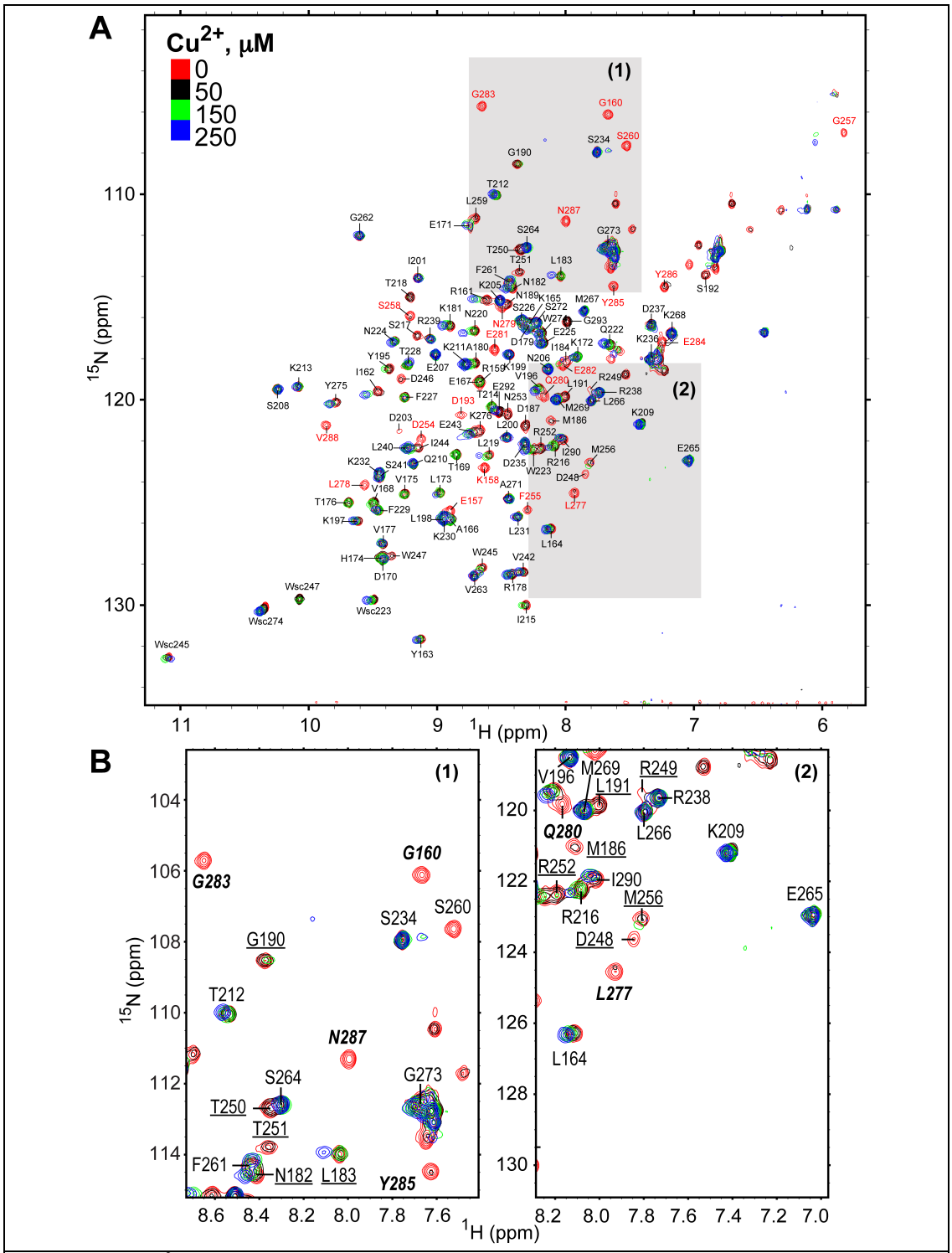

Figure S8. Cu^{2+} binds C2α in the N-terminal/Helix3 and CMBL regions. (A) Overlay of the ^{1}H-^{15}N HSQC spectra of 100 μM C2α at increasing concentrations of Cu^{2+} ions. Residues that broaden beyond detection upon addition of 50 μM Cu^{2+} are labeled in red. (B) Expansions of two regions, (1) and (2), of the same spectrum. Residues that broaden beyond detection upon addition of 50 μM Cu^{2+} are bold/italicized. CMBL residues are underlined.

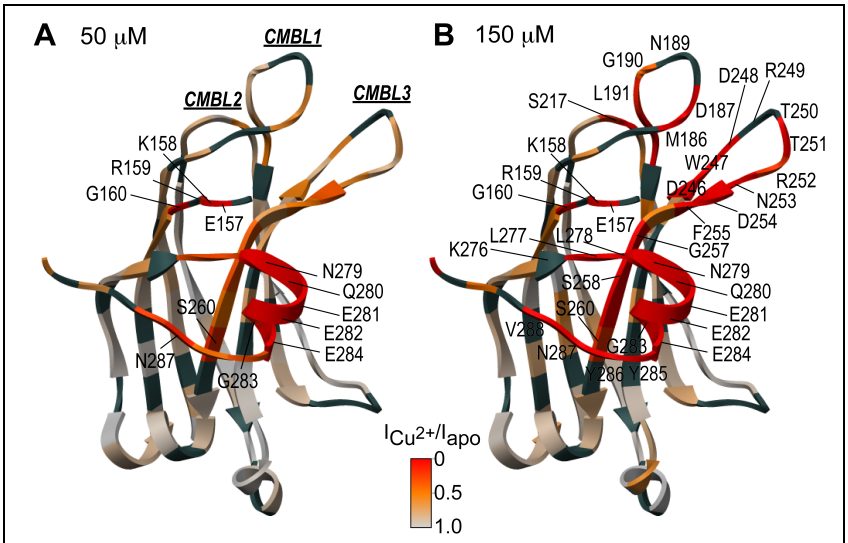

Figure S9. PRE mapping of Cu^{2+} binding sites onto the structure of apo C2α (3RDJ). PRE was calculated as the ratio of cross-peak intensities in Cu^{2+}-complexed C2α to those in apo C2α for two Cu^{2+} concentrations: 50 and 150 μM. The data were normalized to residue K236.

S8. Ultracentrifugation lipid-binding assays.

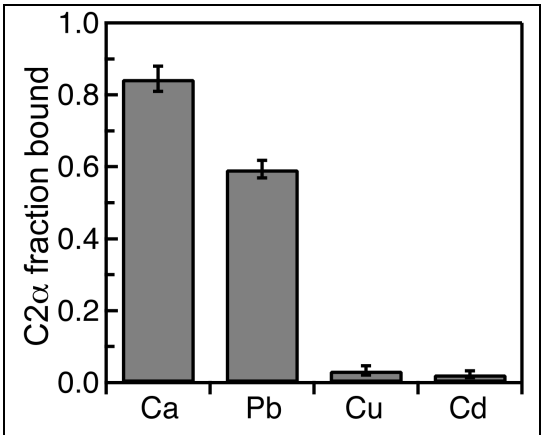

Figure S10. Fractional population of membrane-complexed C2α. Total concentration of C2α and M^{2+} was 5 and 175 μM, respectively. Reducing the amount of PtdSer to 20% virtually eliminates Cu^{2+}-dependent membrane binding of C2α.

The assays were carried out as previously described,[2] at a total lipid concentration of 1.5 mM and C2α concentration of 5 μM. The composition of LUVs was either POPC/POPS (70:30) (**Figure 3C** of the main manuscript) or POPC/POPS (80:20) (**Figure S7 and S10**).

To obtain the data of **Figure S10**, 3 independent ultracentrifugation experiments were carried out for Cd^{2+} and Cu^{2+}; and 2 independent experiments were carried out for Ca^{2+} and Pb^{2+}. For each experiment, the bicinchoninic acid (BCA) assay was conducted to determine the amount of protein in solution. This value was used to calculate the fraction of the protein bound to the LUVs. The error bars of **Figure S10** were calculated as either the standard deviation of the mean fraction bound (Cd^{2+} and Cu^{2+}), or estimated as the difference between the two fraction bound values (Ca^{2+} and Pb^{2+}).

To obtain the data of **Figure 3C** (main manuscript), we conducted two independent binding experiments for each metal ion or metal ion mixture. For each binding experiment, one or two independent BCA assays were done, giving a total of 3-4 measurements per metal ion or metal ion mixture. The error bars of **Figure 3C** were calculated as the standard deviation of the mean fraction bound.

S9. Ca^{2+} displaces Cu^{2+} from the CMBL region of C2α.

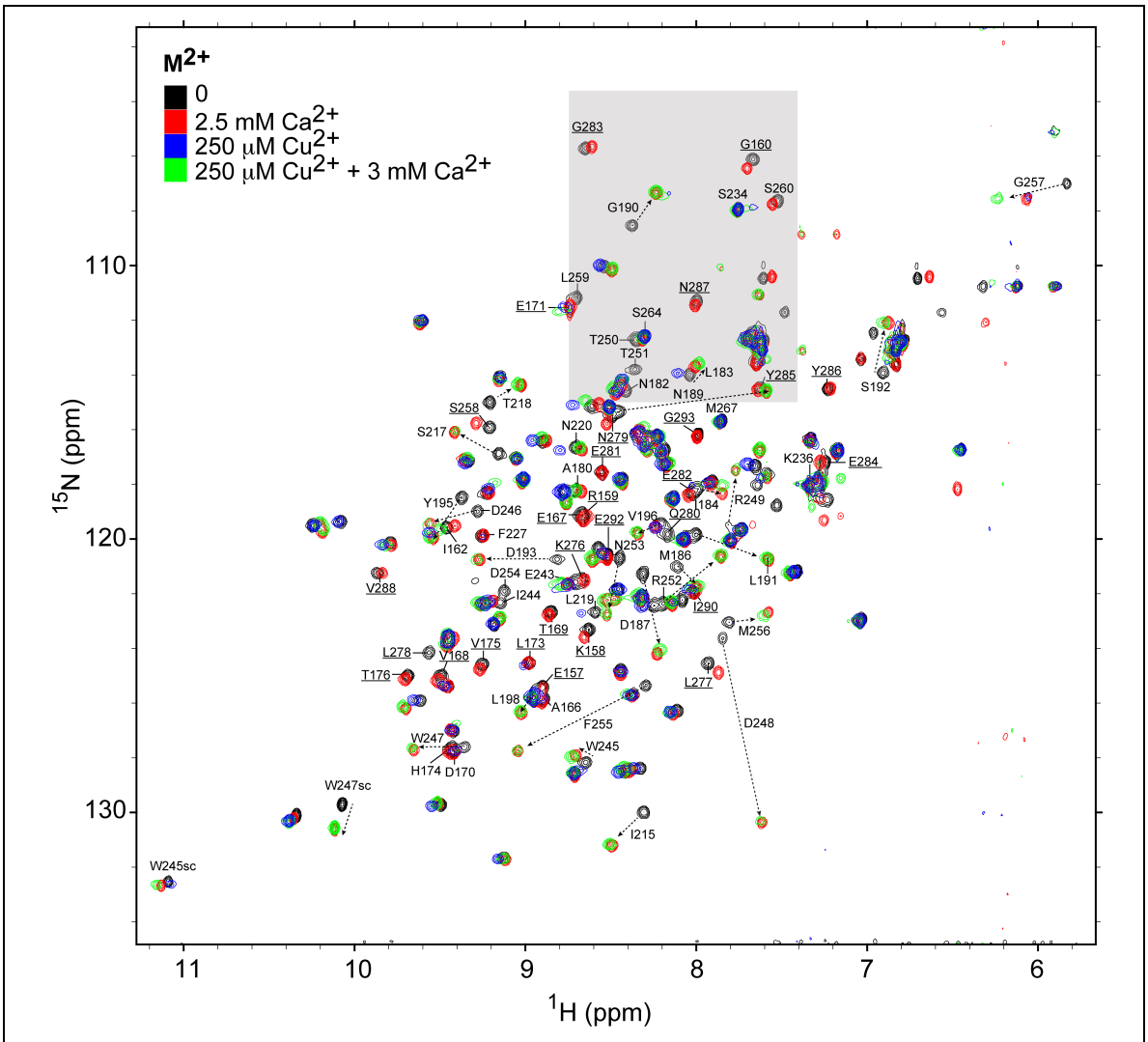

Figure S11. Overlay of the ^{15}N-^{1}H HSQC spectra of 100 μM C2α at several concentrations of Ca^{2+} and Cu^{2+} illustrates the displacement of Cu^{2+} from the CMBL region but not from the N-terminal/Helix3 site. Residues that remain broadened upon addition of 12-fold Ca^{2+} excess over Cu^{2+} are underlined. Residues whose intensity fully recovers upon addition of Ca^{2+} are labeled using regular font. The arrows indicate the direction of the cross-peaks' shift due to Ca^{2+} binding. The shaded region corresponds to the expansion of **Figure 4B** of the main manuscript.

REFERENCES

(1) Lopes, D. H.; Chapeaurouge, A.; Manderson, G. A.; Johansson, J. S.; Ferreira, S. T. *J. Biol. Chem.* **2004**, *279*, 10991.
(2) Morales, K. A.; Lasagna, M.; Gribenko, A. V.; Yoon, Y.; Reinhart, G. D.; Lee, J. C.; Cho, W.; Li, P.; Igumenova, T. I. *J. Am. Chem. Soc.* **2011**, *133*, 10599.
(3) Yamazaki, T.; Lee, W.; Arrowsmith, C. H.; Muhandiram, D. R.; Kay, L. E. *J. Am. Chem. Soc.* **1994**, *116*, 11655.
(4) Schumann, F. H.; Riepl, H.; Maurer, T.; Gronwald, W.; Neidig, K. P.; Kalbitzer, H. R. *J. Biomol. NMR* **2007**, *39*, 275.
(5) Montaville, P.; Coudevylle, N.; Radhakrishnan, A.; Leonov, A.; Zweckstetter, M.; Becker, S. *Protein Sci.* **2008**, *17*, 1025.
(6) Kabsch, W. *Acta Crystallogr. D Biol. Crystallogr.* **2010**, *66*, 125.
(7) Jones, T. A. *Acta Crystallogr. D Biol. Crystallogr.* **2004**, *60*, 2115.
(8) Emsley, P.; Cowtan, K. *Acta Crystallogr. D Biol. Crystallogr.* **2004**, *60*, 2126.
(9) Adams, P. D.; Afonine, P. V.; Bunkóczi, G.; Chen, V. B.; Davis, I. W.; Echols, N.; Headd, J. J.; Hung, L. W.; Kapral, G. J.; Grosse-Kunstleve, R. W.; McCoy, A. J.; Moriarty, N. W.; Oeffner, R.; Read, R. J.; Richardson, D. C.; Richardson, J. S.; Terwilliger, T. C.; Zwart, P. H. *Acta Crystallogr. D Biol. Crystallogr.* **2010**, *66*, 213.
(10) Verdaguer, N.; Corbalán-García, S.; Ochoa, W. F.; Fita, I.; Gómez-Fernández, J. C. *EMBO J.* **1999**, *18*, 6329.
(11) Nalefski, E. A.; Falke, J. J. *Methods Mol. Biol.* **2002**, *172*, 295.